České vysoké učení technické v Praze, Fakulta stavební

Czech Technical University in Prague, Faculty of Civil Engineering

Ing. Pavel Trtík, Ph.D.

Využití synchrotronového záření a soustředěných iontových svazků pro výzkum mikrostruktury cementových past

Use of synchrotron radiation and focused ion beams for investigation of microstructure of cement pastes

Summary

Recent development in the domain of microscopy techniques has enabled the high-resolution 3D imaging of complex, multiphase material microstructures (e.g. those of hardened cement pastes and other materials with inherent sub-microscale structural features). The available techniques for the high-resolution 3D images are presented and their advantages and disadvantages are discussed. In particular, synchrotron micro- & nanotomography and focussed ion beam nanotomography are presented. The use of realistic three-dimensional masks of material phases for the estimation of the local mechanical and other properties of the cement pastes are included in the latter part of the lecture.

Souhrn

Poslední vývoj v oblasti mikroskopických metod umožnil trojrozměrné zobrazování s vysokým rozlišením komplexních, vícefázových mikrostruktur materiálů (např. cementových past a dalších materiálů s inherentní strukturou na submikronové úrovni). Tyto dostupné metody trojrozměrného zobrazování jsou krátce popsány a zároveň jsou uvedeny jejich výhody a nevýhody. Zejména je popsána synchrotronová mikro- a nanotomografie a nanotomografie soustředěného iontového paprsku. V další části přednášky se pojednává o použití realistických trojrozměrných zobrazení materiálových fází pro odhad lokálních mechanických a dalších vlastností cementových past.

Klíčová slova: synchrotron, soustředěný iontový paprsek (FIB), mikrotomografie, nanotomografie, cementová pasta

Keywords: synchrotron, focused ion beam (FIB), microtomography, nanotomography, cement paste

Table of Contents

1. Introduction

In materials science, there is a well-established concept of development of innovations in materials via sound understanding of 'the material structure' vs. 'the material properties' relationships.

Different materials exhibit different 'lengthscales of importance'. The materials based on hydraulic cements do exhibit several of such length scales, with the micro- and nano-scales being the important ones from the point of view of mechanical and transport properties (and hence durability). It was shown (e.g. *Leemann et al. 2010*) that there is a correlation between the properties of bulk cement pastes and overall properties of the cement-based mortars. It is therefore important to understand the properties and hence characterize the properties of the bulk cement pastes. Cement pastes can be considered as the binders of materials summarizingly known as concretes. As the particle sizes of cement usually span the range between about 1 and about 100 micrometers and since the dominant part of porosity of hardened cement pastes has sub-micron dimensions, the characterization of bulk cement pastes is not an easy task. On one hand, the characterization tool should be resolving enough to capture details of microstructure (e.g. bottle-necks in porosity, distribution of hydration products, etc.), with high fidelity, while on the other hand, the characterization tool should allow for investigation of the representative volume elements (RVE) of the material for the purpose of the virtual experiments performed on three-dimensional 3D datasets.

The size of the representative volume element for bulk hardened cement paste can be subject of some debate. However, it is assumed that the RVE of hardened cement pastes is above 100 micrometers. Consequently, the above-mentioned requirements make the characterization of cement pastes a challenging task.

For relatively long time, the electron microscopy has been utilized for characterization of material's microstructure. The electron microscopy has been used extensively also as a tool for assessment of microstructure of hardened cement paste.

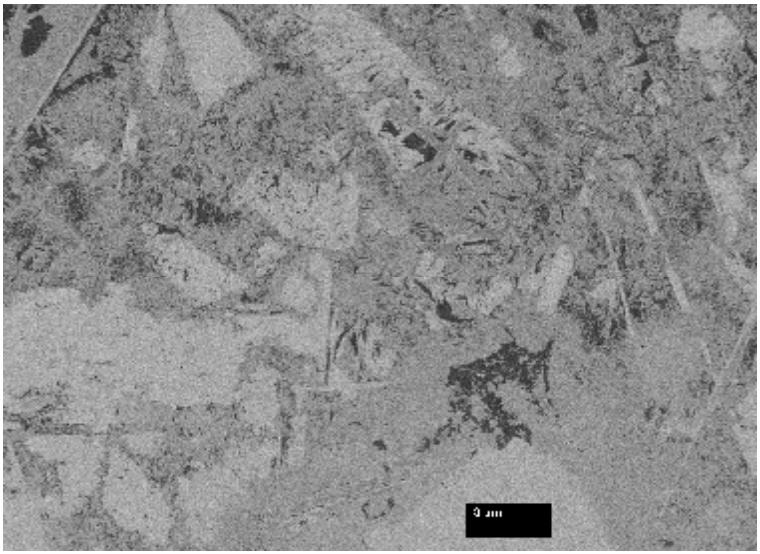

Figure 1 – Low-keV back-scattered electron image of hardened cement pastes. Even though the electron microscopy may provide very high-resolution images the 3D imaging techniques are required so that the true complexity of the material microstructure is revealed.

Figure 1 shows an example of back-scattered electron image of hardened cement paste. Even though the electron microscopy provides a high resolving imaging tool, it can - per se - provide only two-dimensional images of material microstructure.

The microstructure of cement paste is dependent on the original distribution of the unhydrated cement particles and on the arrangement of the hydration products. After mixing of cement powder with water, the hydration products grow from the hydrating cement particles and assemble within the capillary pores. 2D imaging techniques (such as X-ray radiography or back-scattered scanning electron microscopy)

therefore cannot provide full information about the microstructural complexity. Hardened cement pastes, as materials with locally disordered microstructure require therefore three-dimensional characterization tool for the assessment.

3D imaging of materials is also called tomography. Tomography as such is not new; various experimental techniques for three-dimensional reconstructions of microstructures have been successfully utilized in materials science for relatively long time. These techniques include mechanical sectioning and X-ray tomography. Figure 2 shows a diagram that presents some types of tomographies and their respective lengthscales of utilizations.

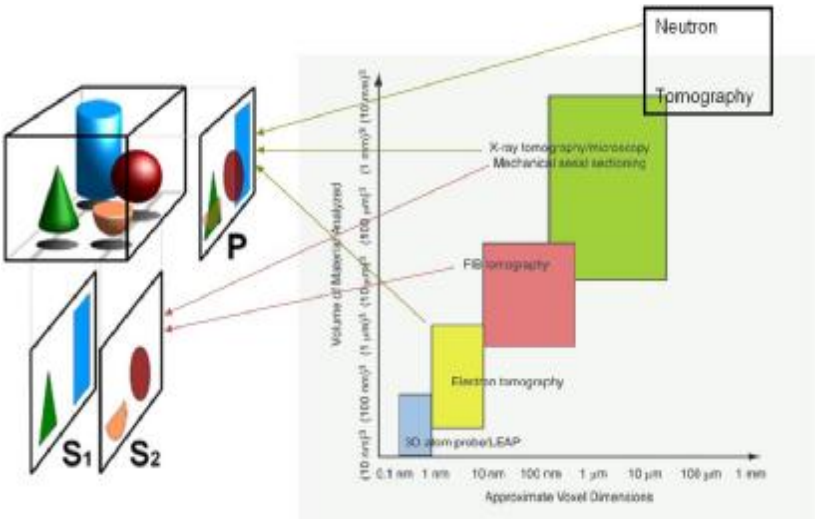

Figure 2 – Diagram showing the distribution of various tomography techniques over several lengthscales. The distinction between tomographies based on projection images (P) and sectioning (S1, S2) is highlighted. Image amended, the original image courtesy of Uchic et al. (2007)

As discussed above, the domain of 3D imaging techniques with length scales resolution about 10-100 nanometers would

be very relevant for investigations of cement-based materials. However, for a long time this lengthscale domain has not been covered by any suitable three-dimensional imaging technique. Relatively recently, this gap in the range of tomographies was bridged by a locally destructive type of tomography based on electron microscopy – focused ion beam nanotomography (FIB-nt). And even more recently, the non-destructive tomography covering these resolutions based on X-rays has been developed and became available at few instruments world-wide as synchrotron nanotomography.

The aim of this presentation is to show several examples in which the tomographies of sub-micron resolutions may provide very useful tools for characterization of properties of cement pastes. The presentation therefore further deals with tomographies based on (i) synchrotron X-rays sources and on (ii) focused ion beam sources. In the later part of the presentation, examples how the acquired 3D datasets can be used for the purpose of some virtual experiments are presented.

2. Tomographies of micro- and nanoscale resolutions

2.1. Synchrotron microtomography

The acquisition of three dimensional images of material microstucture by synchrotron tomography is composed of four principal processes. These are as follows: (i) the generation of X-rays in the synchrotron, (ii) the interaction of X-rays with the investigated sample, (iii) the detection of the X-rays (2D transmission images) in the detector, (iv) the reconstruction of 2D transmission images into the 3D dataset. The above-mentioned procedures are briefly discussed hereinafter.

The X-rays used in the synchrotron tomography are generated in synchrotron facilities. The synchrotrons are specific types of cyclic particle accelerator. In the synchrotron, the accelerated

particles (electrons) are influenced by both an electric and a magnetic field. While the magnetic fields affect the particle trajectories and keep them on a 'closed' polygon path, the electric fields are utilized for the acceleration of the particles. Synchrotron radiation (or synchrotron light) is generated when relativistic electrons undergo a change in the direction in a magnetic field. The synchrotron radiation may cover broad spectrum of energies (wavelengths). However, for the purpose of simplicity, the synchrotron is considered in the following text as the X-ray source only. The quality of synchrotron X-ray source can be expressed by the quantity - *brilliance*. The brilliance of X-ray source is given by the source flux, source size, divergence and monochromaticity. Expressed in brilliance, an undulator (a periodic magnetic insertion device used routinely for production of synchrotron light) is much more powerful device than a rotating anode (source of tabletop X-rays). This fact is one of the principal reasons for utilization of synchrotron radiation for tomographic characterization of materials.

The interaction of the synchrotron radiation (in this case of hard X-rays) can be divided into three categories: photoelectrical absorption, elastic scattering and inelastic scattering. The probability of each of the interactions with the matter can be expressed by the 'process cross-section' and the sum of the three cross-sections is directly proportional to the total linear attenuation coefficient, μ. In the case that the photoelectric absorption prevails (as is the case in the standard absorption tomography), it can be then simplified that the total linear attenuation coefficient expresses the probability that the material will absorb the X-ray photon. It can be shown that the total linear attenuation coefficient is the function of atomic number Z, material density r and radiation energy, E (see Eq. 1).

$$m = r \cdot \left(a + \frac{b \cdot Z^{3.8}}{E^{3.2}} \right) \qquad \text{[Eq. 1]}$$

When considering a beam of a given energy being attenuated by a homogeneous object, the number of photons that interact over a distance *x* is proportional to the number of incident photons according to Beer-Lambert law.

$$I = I_0 \cdot \exp(-m \cdot x) \qquad \text{[Eq. 2]}$$

In the end, the X-rays generated by a source and attenuated by the sample are collected at a detector. The schematic diagram of the synchrotron tomography test set-up with a detector is shown in Figure 3.

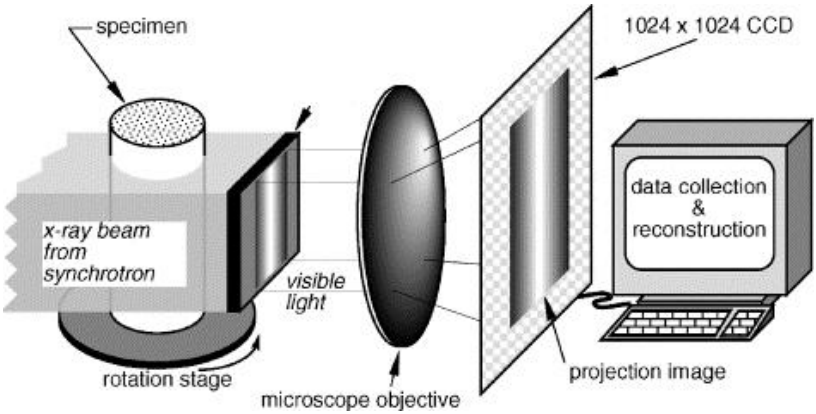

Figure 3 – The schematic diagram of the synchrotron tomography test arrangement. The resolution of this arrangement is limited by conversion of the X-rays into visible light using scintillator. Amended, original image courtesy of Landis et al. (2003)

In Figure 3, the X-rays are coming from the source placed far left and are attenuated by the specimen. The efficiency of most photon detectors is rather low in the X-ray regime. Therefore,

scintillators are required to convert the X-rays to visible light. It is indeed this process that seriously limits the resolution of the standard absorbtion-based synchrotron microtomography at about one micrometre. Usually some optical elements, such as mirrors and lenses, are utilized to divert the visible light onto a detector. The two-dimensional charge-coupled devices consisting of large number of detector elements are usually used as detectors.

Computed tomography is the three-dimensional imaging of an object from two-dimensional transmission images by illuminating the given object from many different angular positions. Synchrotron X-ray tomography is from this point of view one of the techniques in the family of computed tomographies. The advantage of synchrotron tomography over standard X-ray tomography lies in the powerful source of the X-rays with close-to-parallel beam geometry.

The number of projections should fulfill the sampling theorem, in which X is required number of projections and Y is the number of points that sample on single projections (see Eq. 3).

$$X = \frac{p}{2} \cdot Y \qquad \text{[Eq. 3]}$$

In other words, the tomographed object should be captured by X transmission images (projections) of Y pixels in width to fulfil the sampling theorem. The task of absorption-based computed tomography is to reconstruct the distribution of the linear attenuation coefficient $\mu(x,y)$ in the object. For this purpose, the intensities collected in all the detector elements and for all the captured projections are collected in the sinograms $p_z(d,q)$.

In order to solve this question a transformation from $p_z(d,q)$ to $\mu(x,y)$ is required. The opposite transformation (i.e. from a function $\mu(x,y)$) to its parallel beam projection form is called the Radon transform. Therefore, the reconstruction of $\mu(x,y)$ from the sinogram $p_z(d,q)$ can be performed by the inverse Radon

transform. As the inverse Radon transform would work perfectly only for q varying continuously between 0 and π, the filtered back projection algorithm (*Kak & Slaney, 1988*) is utilized in practice.

There are ample investigations that utilize the (synchrotron) X-ray microtomography for investigation of various materials and number of in-situ (synchrotron) X-ray tomography studies of microstructure of engineering materials were performed (e.g. *Beckmann et al., 2007*) The potential of X-ray microtomography for materials science has been published by Stock (*Stock, 1999*) and since then the research in this domain has progressed significantly. Regarding the investigations of microstructure of hardened or hardening cementitious materials, a number of publications became available in the last decade (e.g *Bentz et al., 2002*; *Gallucci et al., 2007*, *Promentilla et al., 2009*). Synchrotron X-ray microtomography can provide 3D representation of the material microstructure non-invasively and therefore in-situ experiments revealing an evolution of material microstructure can be performed. For cementitious materials, in-situ investigations revealed progression of sulphate attack on cement paste (*Stock et al., 2002*), the evolution of hydration products in early age cement pastes (*Helfen et al., 2005*), the fracture processes (*Landis et al., 2003*, *Trtik et al., 2007*), etc. The synchrotron microtomography can also provide information on the changes in the pore structure of cement pastes due to drying. In all above-mentioned cases, however, the resolution of the microtomography experiments did not trespass the isotropic barrier of 1 μm^3.

2.2. Synchrotron nanotomography

As was mentioned above, the spatial resolution of synchrotron microtomography is limited by the arrangement of the X-ray detector. This limit is usually stated to be about 1 micrometre. In order to trespass this barrier and reach the resolutions below 100 nanometres, the use of other type of test

arrangement is required. Such test arrangement can be based on the use of magnifying X-ray optics and only few instruments worldwide can tackle this challenging task (mostly in soft X-ray regime).

As the penetration capability of the soft X-rays is rather low, the thickness of the samples that can be investigated is seriously limited. The synchrotron nanotomography end-station that utilizes hard X-rays has been recently developed at the beamline for Tomographic Microscopy and Coherent Radiology Experiments (TOMCAT) of the Swiss Light Source (Swiss synchrotron facility). The full-field X-ray instrument - that operates at 10 keV photon energy - can efficiently record tomographic images at measured three-dimensional spatial resolution of 144 nm base on both (i) absorption and (ii) phase contrast.

In order to investigate the material microstructure with such a high-resolution, the thickness of the samples has to be intrinsically limited. At this photon energy and utilized thicknesses of the investigated samples (below 100 micrometres), the low absorbing materials create significant phase shift of the incoming x-ray radiation that can be detected and used for imaging of material microstructure.

A range of phase sensitive techniques exists for full-field x-ray microscopes. These techniques include Zernike and differential phase contrast imaging methods. Zernike phase contrast microscopes (used originally in the light microscopy) utilize hollow cone illumination and an imaging lens in combination with a separate $\pi/2$ phase ring that is placed in the back-focal plane of the imaging lens. The size of the phase ring has to match the geometry of the undiffracted light from the sample and the modulation of the intensity arises from the fact that the phase between the diffracted wave front and the undiffracted one is shifted. The details of the operating principle and of the test arrangement at TOMCAT were published recently (*Stampanoni et al, 2010*).

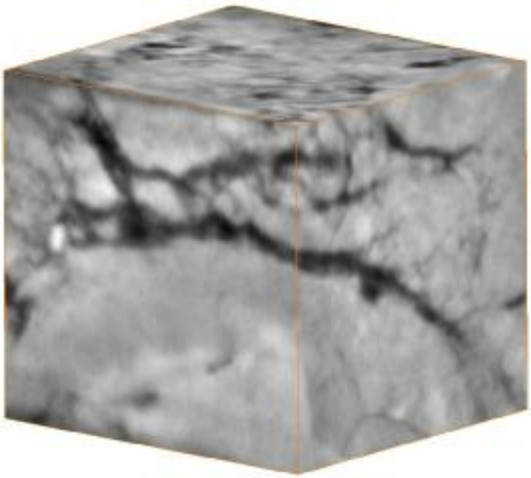

Figure 4 - Image of the three-dimensional dataset of epoxy-impregnated hardened Portland cement paste based on synchrotron phase-contrast X-ray nanotomography. The size of the dataset is 283 x 283 x 304 voxels, the isometric voxel size equals 53.6 nm.

It needs to be highlighted here that the X-ray nanotomography experiments are rather novel and still relatively rare and only very few instruments in the world (predominantly installed at 3rd generation synchrotron X-ray sources) can trespass the isotropic resolution barrier of 100 nanometres. The recently acquired datasets of hardened cement paste (see Figure 4) that is based on phase-contrast X-ray nanotomography, is to the best of author's knowledge one of the first 3D images of hardened cement paste with decananometre voxel resolution based on a non-destructive technique.

2.3. Focused ion beam nanotomography

Focused ion beam nanotomography (FIB-nt) is, in principle, nanoscale material sectioning that utilizes ion beams for removal of well-defined volumes of material.

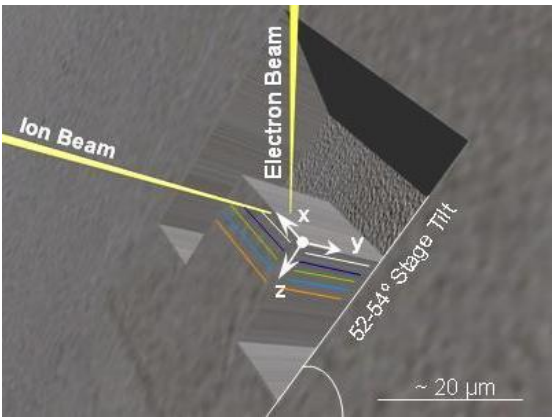

Figure 5 – Diagram showing the distribution of various tomography techniques over several lengthscales. The distinction between tomographies based on projection images and sectioning is highlighted. Image amended, the original image courtesy of Holzer et al. (2004)

Gallium (or possibly other element) ion beam is used in the commercially available microscopes for the erosion of thin layers of material. A stack of electron images is acquired as shown schematically in Figure 5.

For the cementitious materials, FIB-nt technique was hitherto utilized for investigation of particle size distribution and morphology of cement particles (*Holzer et al. 2006a*; *Munch et al., 2006*), morphology and spatial arrangement of early hydration products (*Holzer et al., 2007*) and nanoscale porosity (*Holzer et al. 2006b*; *Munch & Holzer 2008*). It should be mentioned here that (i) FIB-nt is locally destructive imaging technique; (ii) the voids in the porous media to be investigated by FIB-nt need to be filled (impregnated) by a matter (usually epoxy resin). To what extent this sample preparation procedure alters the micro/nanostructure from the pristine conditions needs to be investigated in the future experiments.

In principle, the FIB-nt procedure consists of three rather independent steps:

- erosion of material in closed vicinity of the selected

region of interest

- ion beam sectioning and electron beam imaging (Slice and View)
- data processing of the acquired electron microscopy images.

The recent advances in the FIB-nt instrumentation allow for the acquisition of realistic three-dimensional images of material microstructure. An example of such a 3D dataset based on FIB-nt is shown in Figure 6. Realistic three-dimensional mask of mask of porosity can be segmented from such an 3D image.

Figure 6 - Three-dimensional dataset of hardened Portland cement paste based on focussed ion beam nanotomography (FIB-nt). The isometric voxel size is 20 nm, leading to the corresponding size of the dataset of 35.2 x 26.5 x 32.0 μm^3.

3. Examples of utilization of high-resolution 3D images for the investigations of cement pastes

On successful 3D segmentation of the dataset into material phases (e.g. in the case of hardened cement pastes into porosity, hydration products, unhydrated residues of cement particles, etc.), the virtual experiments on hardened cement pastes can be performed. This chapter presents two examples in which high-resolution 3D images are used for assessment of

properties of hardened cement pastes.

In the first example, the high-resolution 3D image of hardened cement paste is utilized for virtual topographic experiment (*Trtik et al., 2008*) from which the surface roughness of hardened cement paste is analyzed. The surface roughness affects the results of nanomechanical tests. The surface roughness values to be measured on a surface of a porous material are dependent on the properties of the naturally occurring pore space. In order to assess the surface roughness of hardened cement paste without the actual influence of the usual sample preparation for nanomechanical testing (i.e. grinding and polishing), 3D datasets were utilized for reconstruction of 3D (nanoscale resolution) surface profiles of hardened cement pastes. The resulting root mean square surface roughness (between 115 and 494 nm) was considerably higher than some roughness values (as low as 10 nm) reported in the literature.

In the second example, the high-resolution 3D image of hardened cement paste serves as a valuable input for virtual experiment (*Trtik et al., 2009*) that emulates statistical nanoindentation. In the experiment, a marching object was sampled over a large number of positions. Based on the local phase composition within the marching object, a local stiffness was estimated by using simple composite models. Due to the large number of the investigated positions, the elastic modulus was statistically evaluated in the same manner as in real statistical indentation experiment. The results reveal that the elastic modulus histograms show multiple peaks even in the case of a material that is segmented into three phases only (porosity, hydrated and unhydrated phases), i.e., without the hydrated phase being composed of different types of distinct hydration products. The presented results question the notion that the multipeak signature in the statistical nanoindentation experiments on HCP can be explained only by the presence of two distinct C–S–H phases.

4. Bibliography

Beckmann F., Grupp R., et al., Adv. Eng. Mater. 9 (2007) 939

Bentz, D.P., Mizell, S., et al. J. Res. Nat. Inst. Standard. Technol. 107 (2002) 137

Gallucci E., Scrivener K., et al., Cem. Concr. Res. 37 (2007) 360

Helfen L., Dehn E., et al., Adv. Cem. Res. 17 (2005) 103

Holzer, L., Muench, B., et al., J. Am. Ceram. Soc. 89 (2006) 2577

Holzer L., Gasser P., et al., J. Microsc. 227 (2007) 216

Holzer L., Gasser P. & Munch B. Proc. ECF 16 (2006)

Kak A.C. & Slaney M., IEEE Press (1988)

Landis E.N., Nagy E.N. & Keane D.T., Eng. Fract. Mech., 70 (2003) 911

Leemann A., Loser R., et al., Cemsuisse project 201002, (2010)

Munch B., Gasser P., et al., J. Am. Ceram. Soc. 89 (2006) 2586

Munch B. & Holzer L., J. Am. Ceram. Soc. 91 (2008) 4059

Promentilla M. A. B., Sugiyama T., et al., Cem. Concr. Res. 39 (2009) 548.

Stock S.R., Int. Mater. Rev. 44 (1999) 141

Stock S.R., Naik N.K., et al., Cem. Concr. Res. 32 (2002) 1673

Stampanoni M., Mokso R., et al., Phys. Rev B (2010)

Trtik, P., Stahli, P., et al., FraMCoS-3 (2007) 1277

Trtik P., Dual J., et al., J. Microsc. 232 (2008) 200

Trtik P., Munch B. & Lura P., Cem. Concr. Comp. 31 (2009) 705

Uchic M.D., Holzer L, et al., MRS Bull., 32 (2007) 408

5. Ing. Pavel Trtik, Ph.D. – Curriculum vitae

Personal data:

Date of birth: 19th January, 1973

Nationality: Czech

Marital status: married

Home address: Keferholzstr.151,8046Zürich, Switzerland

E-mail: pavel.trtik@empa.ch, ptrtik@gmail.com

Studies & Employment:

2008 – present:

Scientist, Laboratory for Cement and Construction Chemistry, EMPA Materials Science Technology, Dübendorf, Switzerland.

2006 – 2008:

Research Assistant, Centre of Mechanics (Group Prof. J. Dual), ETH Zurich, Switzerland.

2003 – 2006:

Research Assistant, Institute for Building Materials (Group Prof. van Mier), ETH Zurich, Switzerland.

2000 - 2002:

Research Assistant/Project Leader, Scottish Centre for Nanotechnology in Construction Materials, Advanced Concrete and Masonry Centre, University of Paisley.

1997 - 2000:

PhD Research Student, Department of Civil, Structural and Environmental Engineering, University of Paisley, under supervision of Prof. Peter J. M. Bartos.

1991 - 1997:

Full-time Student, Czech Technical University, Faculty of Civil Engineering, Prague. Final project supervised by Assoc. Prof. Vl. Hrdoušek